

1 **Investigation of the fire mass loss rate in confined and mechanically ventilated enclosures**  
2 **on the basis of a large-scale under-ventilated fire test**

3 Hugues Prétrel<sup>a\*</sup>, Sylvain Suard<sup>a</sup>

4 <sup>a</sup>Institut de Radioprotection et de Sûreté Nucléaire, Centre de Cadarache, Bâtiment 346, 13115 St  
5 Paul Lez Durance, France

6 \*Corresponding author: hugues.pretrel@irsn.fr

7 **Highlights:**

- 8 • Under-ventilated combustion regimes in mechanically ventilated enclosures
- 9 • Effect of oxygen vitiation on the burning rate
- 10 • Summary analysis from a large-scale fire test database
- 11 • Application to complex scenarios representative of real fires event

12 **Abstract:**

13 This study concerns the under-ventilated combustion regimes of a fire scenario in mechanically  
14 ventilated enclosures. Using the theoretical approach of the well-stirred reactor model and the  
15 data-base of large-scale pool fire tests, the study analyses the mass loss rate as a function of the  
16 environmental conditions. The novelties lie in the analysis of a large set of realistic scenarios  
17 involving complex geometries (several compartment connected) and new ventilation  
18 configurations and the applicability of the well-stirred reactor model to interpret these scenarios.  
19 The variables of interest are the combustion regimes (stationary, transient or with rapid  
20 quenching), the duration of the combustion phase and the mass loss rate. The results show a  
21 satisfactory prediction of the well-stirred reactor model to interpret the experimental results of  
22 complex and realistic fire scenario and the robustness of this model to deal with the under-  
23 ventilated regimes. The analysis also highlights the interest of two new parameters rarely used in  
24 the literature, the ventilation factor and the mass factor, to characterise under-ventilated  
25 scenarios. The analysis points out the importance of the relationship expressing the burning rate  
26 as a function of environmental conditions (oxygen level and external flux) and extinction  
27 conditions.

28 **Keywords:** compartment fires; burning rate; under-ventilated, combustion regimes

29 **1 Introduction**

30 Compartment fires remain an important safety issue for the assessment of fire risk in nuclear  
31 facilities. These events, often encountered in nuclear installations and more generally in the  
32 industrial area, presents the particular feature of a strong coupling between the fire heat release  
33 rate and the environment. The physical understanding and the numerical simulation of these  
34 scenarios require appropriate modelling of the fire heat release rate, and the induced flows  
35 generated such as the thermal plume, ceiling jet and smoke filling. In terms of modelling, a

36 scientific bottleneck of these fire scenarios lies in the quantification of the coupling between the  
37 burning rate and the environment, which is rapidly vitiated by gaseous combustion products and  
38 soot and characterized by high temperature. The coupling between the fire and the environment  
39 leads to different combustion regimes such as stationary, oscillatory, or transient to rapid  
40 extinction. The nature of these different regimes depends on the thermodynamic conditions  
41 surrounding the fire, in particular the oxygen concentration and the temperature of the gases as  
42 well as the presence of combustion products (CO and soot). The literature on compartment fires  
43 is very extensive and a large proportion of it concerns natural ventilation with openings to the  
44 outside (i.e. façade fire applications). The configuration of an enclosure ventilated only by  
45 mechanical ventilation has been less extensively addressed but remains a configuration of  
46 interest especially for applications in the nuclear industry.

47 One of the first studies for mechanically ventilated configurations was that of Peatross & al.  
48 showing from a medium-scale 34 m<sup>3</sup> single compartment tests with pool fires and solid fuel  
49 (PMMA) that there is a linear dependence of the mass loss rate (MLR) and the oxygen  
50 concentration in the vicinity of the fire [1]. This work was continued during the three PRISME  
51 research programs (PRISME, PRISME2 and PRISME3) led by the French “Institut de  
52 Radioprotection et de Sûreté Nucléaire” in the framework of the Organisation for Economic Co-  
53 operation and Development (OECD/NEA) on more complex configurations involving several  
54 compartments of 120 m<sup>3</sup> and 170 m<sup>3</sup> connected together with openings [2],[3] [4]. Among other  
55 conclusions, these projects showed that the fire heat release rate is often lower than that in an  
56 open environment due to a change in the environment, particularly the decrease of the oxygen  
57 content. Other studies highlighted the specific feature of fires in a mechanically ventilated  
58 enclosure that can lead to unstable or oscillatory regimes [5], [6], [7], [8]. These large-scale  
59 observations were confirmed by academic studies carried out on a smaller scale, allowing a  
60 wider range of parameters and more detailed metrology[9] (8 m<sup>3</sup> compartment), [10] (1.9 m<sup>3</sup>  
61 compartment), [11] (1 m<sup>3</sup> compartment), and [7] (0.2 m<sup>3</sup> compartment). The influence of the  
62 position of the air vents on the fire heat release rate was also addressed by [12], [13] (8 m<sup>3</sup>  
63 compartment), [14] (25 m<sup>3</sup> compartment). Oscillatory regimes were further demonstrated for  
64 different configurations [15] [16]. Studies with controlled atmosphere cone calorimeter were also  
65 able to show the dependence of the MLR on the oxygen concentration for liquid pool fires and  
66 PMMA plates [17]. More recently, attempts to reproduce a given one compartment large-scale  
67 fire scenario (120 m<sup>3</sup> compartment) at small-scale (1.9 m<sup>3</sup> compartment) were performed  
68 successfully and demonstrated the performance of down-scaling mechanical ventilated fire  
69 scenario [18]. This reduced scale approach was also considered to demonstrate the relevance of  
70 the well-stirred reactor (WSR) approach in ranking and characterizing the combustion regimes  
71 for dodecane pool fire in a single mechanically ventilated compartment [10].

72 The purpose of the present study is to consider the analysis developed in [10] for a simple  
73 configuration (single compartment of 1.9 m<sup>3</sup>) to interpret a wide spectrum of more realistic and  
74 complex fire scenario and to discuss how the behaviour reported at reduced scale remains  
75 applicable for real situations. These scenarios are those investigated experimentally in the  
76 framework of the three PRISME projects that include several compartments of various  
77 dimensions (120 m<sup>3</sup> to 170 m<sup>3</sup>) connected to each other by doorways or vents and representative  
78 of scenarios encountered in nuclear facilities. Some of these tests have already been analysed

79 separately, focusing on a particular aspect of the scenario, influence of doorway [19], vent [20]  
 80 or ventilation flow rate [21]. The novelty of this work lies in highlighting the applicability of the  
 81 WSR model for interpreting the behaviour of fire scenarios in complex configurations such as  
 82 those encountered in real-life situations. It highlights the generic nature of analyses developed on  
 83 a reduced scale or on simplified configurations. This work also makes it possible to bring  
 84 together in a review study a very varied set of large-scale and representative tests. First, the  
 85 analytical means implemented for this study are recapped. This concerns the basis of the WSR  
 86 approach as well as the fire test data-base. The analysis of the results is then presented by  
 87 focusing on the evolution of the MLR in time, the duration of the combustion phase and the  
 88 dependence of the environmental conditions on the MLR.

## 89 2 Material and methods

### 90 2.1 Summary of the well stirred reactor (WSR) model

91 The following is a recap of the WSR approach, often considered for compartment fire analysis  
 92 [22] [23], [24], and applied in the present work to analyse the change in MLR. This approach,  
 93 revisited recently in [10], considers the fire compartment as a homogeneous reactor in which  
 94 oxygen and gaseous fuel interact, leading to an exothermic reaction. As previously derived in  
 95 [10], the oxygen mass conservation in its raw form is

$$96 \frac{d}{dt}(\rho_o V y_{O_2}) = (y_{O_2}^o - y_{O_2})\dot{m}_v - r \cdot \dot{m}_f \quad (1)$$

97  $\rho_o$  and  $V$  are the gas density in the compartment assumed to be constant and the compartment's  
 98 volume respectively.  $y_{O_2}^o$  and  $y_{O_2}$  are the average mass fraction in the air (0.23) and in the  
 99 compartment respectively,  $\dot{m}_v$  is the ventilation flow rate assumed to be constant,  $r$  is the  
 100 stoichiometric ratio and  $\dot{m}_f$  the MLR that may vary with time. This balance states that the  
 101 variation in oxygen in the compartment depends the oxygen supply through ventilation and the  
 102 oxygen consumption by the fire. A dimensionless form is expressed in order to identify the  
 103 ventilation factor as :

$$104 \frac{d}{d\tau} Y = (1 - Y) - \phi_o M \left( \frac{Y_{O_2}^o}{r} Y + 1 \right) \quad (2)$$

105 where  $Y = y_{O_2}/y_{O_2}^o$  is the dimensionless average mass fraction of oxygen,  $\tau = \dot{m}_v/(\rho_o V) \cdot t$  the  
 106 dimensionless time. This approach highlights the importance of the MLR and the ventilation  
 107 flow rate integrated through a single parameter, the ventilation factor,  $\phi_o = r\dot{m}_f^o/y_{O_2}^o\dot{m}_v$ . This  
 108 parameter, similar to the global equivalence ratio (GER), expresses a ratio of oxygen mass flow  
 109 rates: one required to burn the fuel in open atmosphere and one injected into the compartment by  
 110 the ventilation. One feature of this definition is to only consider variables known before the  
 111 experiment ( $\dot{m}_f^o$  and  $\dot{m}_v$ ). The ventilation factor allows the type of combustion to be ranked as  
 112 well-ventilated ( $\phi_o \ll 1$ ) or under-ventilated ( $\phi_o \gg 1$ ). A value of one corresponds to a balance  
 113 between the oxygen demand through combustion and the oxygen supply through ventilation. The  
 114 model also introduces the dimensionless MLR as  $M = \dot{m}_f/\dot{m}_f^o$  where  $\dot{m}_f^o$  is the reference one in  
 115 open atmosphere. It is worth noting that this approach of the WSR model is limited in the present

116 analysis to the mass balance and does not include the energy balance, which allows the temporal  
 117 evolution of temperature to be expressed. This choice simplifies the presentation but has no  
 118 influence on the conclusions that can be drawn from the model. The WSR approach may also  
 119 highlights the influence of the gas conditions in the compartment (oxygen concentration and  
 120 temperature) on the MLR. In this case, the MLR is no more a fixed input parameter but varies  
 121 with time as the oxygen concentration and the gas temperature. They are many laws that can be  
 122 considered and one of these is the following one used in [10]:

$$123 \quad M = (1 - M^e)[(Y - Y^e)/(1 - Y^e)] + M^e \quad (3)$$

124 where  $M^e$  and  $Y^e$  are the dimensionless MLR and oxygen mass fraction at extinction (equivalent  
 125 to the low oxygen index, LOI). Relation (3) expresses a linear relationship between the MLR and  
 126 the oxygen concentration. It states that the reduction of the oxygen concentration will  
 127 proportionally reduce the radiation from the flame towards the combustible and thus the MLR.  
 128 The parameters  $M^e$  and  $Y^e$  express the boundary conditions at extinction. The relations (2) and  
 129 (3) are solved numerically to obtain the dimensionless time evolution  $M(\tau)$  and  $Y(\tau)$ , for which  
 130  $\phi_o$ ,  $r$ ,  $M^e$  and  $Y^e$  are parameters. A variable of interest for ranking the combustion regimes is the  
 131 time to extinction (or the duration of the combustion period), ending either through lack of fuel  
 132 or lack of oxygen. Its determination is therefore based on two cases: (1) the dimensionless  
 133 oxygen fraction reaches the LOI,  $Y(\tau) = Y^e$  or (2) the time integral of the dimensionless MLR is  
 134 equal to a dimensionless mass  $m^*$ ,  $\int_0^\tau M d\tau = m^*$  and extinction occurs through lack of fuel. For  
 135 the second case, the parameter  $m^* = [(rm_f^{init})/(y_{O_2}^o \rho_o V)]/\phi_o$  includes the initial mass of fuel,  
 136  $m_f^{init}$ . A dimensionless time to extinction is defined as  $t_{ext}^* = t_{ext} \dot{m}_f^o / m_f^{init}$  to get rid of the  
 137 initial mass of fuel. It is worth noting that the dimensionless mass  $m^*$  contains a second  
 138 important ratio, the mass factor  $\phi_m = (rm_f^{init})/(y_{O_2}^o \rho_o V)$ : the mass of oxygen required to  
 139 oxidize the total mass of fuel divided by the mass of oxygen initially in the compartment's  
 140 volume. This parameter is an important characteristic of the fire scenario. For a low value of  $\phi_m$   
 141 (low fuel mass in a large volume for instance), all the fuel is consumed before reaching the  
 142 conditions of extinction through lack of oxygen and the scenario is therefore not affected by  
 143 extinction conditions, whatever the ventilation flow rate.

144 An example calculation is given in Fig. 1 to illustrate the influence of the model parameters. The  
 145 evolution with time of the oxygen concentration (Fig. 1 a and b) is presented for several values  
 146 of the ventilation factor  $\phi_o$  and for two given values of  $\phi_m$  (0.2 and 0.6). For a low value of  $\phi_m$   
 147 (here 0.2, Fig. 1-a), the conditions for extinction through lack of oxygen are never met and the  
 148 extinction always occurs through lack of fuel. For a higher value of  $\phi_m$  (here 0.6 Fig. 1-b), both  
 149 extinction modes are encountered, depending on the value of the ventilation factor. In the latter  
 150 case, the duration of the combustion phase first increases with  $\phi_o$  for low values of  $\phi_o$  (0.1 and  
 151 0.4) and extinction occurs here through lack of fuel. Then, for higher values of  $\phi_o$ , (1 and 2), the  
 152 opposite behaviour is observed: the duration of the combustion phase decreases with  $\phi_o$   
 153 (extinction occurs by reaching the LOI).

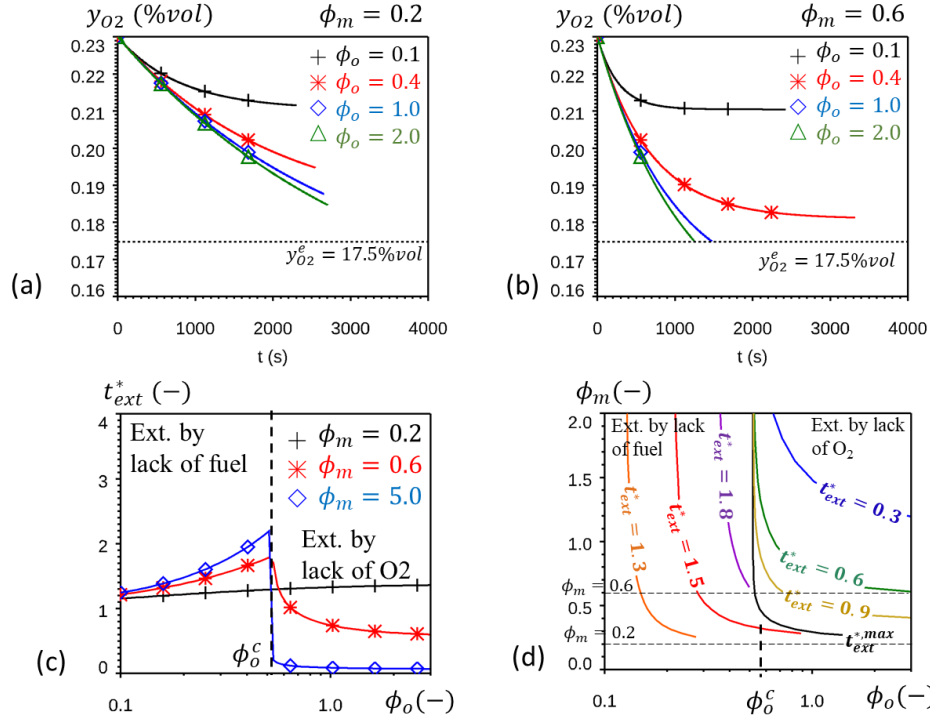


Fig. 1. Examples of simulation with the WSR model (where  $M^e=0.44$  and  $Y^e=0.76$ ) (top) time variation of O<sub>2</sub> concentration with  $\phi_m = 0.2$  (a) and with  $\phi_m = 0.6$  (b)- (Bottom)  $t_{ext}^*$  versus the ventilation factor  $\phi_o$  for three values of  $\phi_m$  (c), Iso-contours of  $t_{ext}^*$  in the  $(\phi_m, \phi_o)$  domain (d).

154 The evolution of  $t_{ext}^*$  as a function of  $\phi_o$  is summarized in Fig. 1-c for three values of  $\phi_m$ . For  
155 values of  $\phi_m$  above or equal to 0.6, the two opposite behaviours mentioned previously are  
156 observed:  $t_{ext}^*$  first increases with  $\phi_o$  due to a decrease in the MLR (under the effect of oxygen  
157 reduction) and an oxygen concentration still above the LOI due to a high ventilation rate in  
158 comparison to the MLR (low  $\phi_o$ ). At  $\phi_o$  above a critical value, the reverse behaviour is  
159 evidenced:  $t_{ext}^*$  decreases because the LOI is reached faster with a ventilation rate too low  
160 compared to the MLR. Fig. 1-c and Fig. 1-d also illustrate the behaviour for scenarios with low  
161  $\phi_m$  (here 0.2) for which only one regime is observed. Extinction occurs only due to lack of fuel  
162 (the conditions for extinction through lack of oxygen are never encountered) because of too little  
163 fuel mass in a very large volume. As previously derived in [10], the critical ventilation factor  
164  $\phi_o^c = (1 - Y^e)/M^e(1 + y_{O_2}^o/r Y^e)$  that characterizes the change of behaviour (only for  
165 scenarios with  $\phi_m$  large enough) only depends on the extinction conditions specified here with  
166 the parameters  $M^e$  and  $Y^e$ . The WSR model gives the basis to characterize the combustion  
167 regimes based on the fire duration, the extinction mode, the ventilation factor and the mass factor  
168  $\phi_m$ . These parameters will be considered to analyse the burning rate in large-scale fire  
169 experiments.

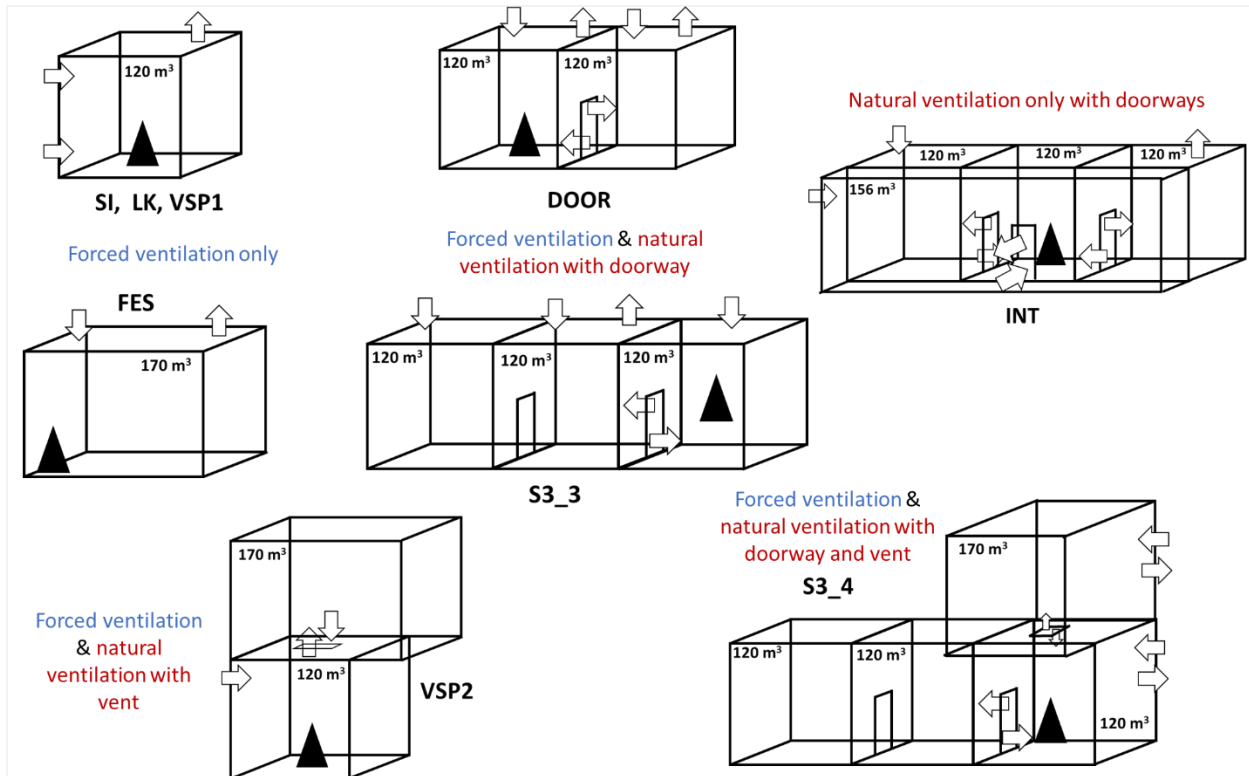


Fig. 2. Illustration of the configurations with various types of ventilation considered in the data-base (arrows indicate the air flows).

## 170 2.2 Fire experiments

171 The fire experiments considered in this study concern scenarios involving an hydrocarbon pool  
 172 fire in various configurations of mechanically ventilated compartments. These tests were carried  
 173 out at IRSN's DIVA facility as part of the OECD/NEA PRISME projects. The special feature of  
 174 these tests is that they produce a wide variety of ventilation configurations that are barely  
 175 discussed in the literature. They were carried out during several experimental campaigns (named  
 176 SI, DOOR, LK, INT, VSP1, VSP2, FES, S3\_3 and S3\_4, acronyms used in the project and the  
 177 related publications), each with a specific configuration of the experimental set-up as shown in  
 178 Fig. 2. The first configuration concerns a ventilated, single compartment  $120\text{ m}^3$  by volume (SI,  
 179 LK and VSP1 series), or  $170\text{ m}^3$  by volume (FES series). The second configuration involves two  
 180 compartments connected via a doorway (DOOR series), or by a vent (VSP2 series). The third  
 181 configuration involves three compartments connected via doorways (S3\_3 series). Finally, a  
 182 fourth configuration involves four compartments connected via doorways (INT) or via doorways  
 183 and a vent (S3\_4 series). For all tests, the fire compartment's volume is  $120\text{ m}^3$  or  $170\text{ m}^3$ . The  
 184 fire compartment had various ventilation configurations: (i) only mechanical ventilation (SI, LK,  
 185 FES and VSP1), (ii) only natural ventilation via doorways (INT), (iii) mechanical and natural  
 186 ventilation via doorways and/or vents (DOOR, VSP2, S3\_3 and S3\_4). The mechanical  
 187 ventilation is provided through an inlet positioned at the top of the compartment except for the SI  
 188 series in which two tests had inlets at the bottom of the compartment. The natural ventilation is  
 189 provided by the incoming air through an opening: (i) a vertical doorway (INT, DOOR), (ii) an

190 horizontal vent (VSP2) or both (S3\_3 and S3\_4). The ventilation rate (or air change per hour  
 191 ACH) is calculated based on the air flow rate supplied by the mechanical ventilation duct only  
 192 and the volume of the fire compartment (120 m<sup>3</sup> or 170 m<sup>3</sup>).

193 In all fire tests, the fire is a circular pool fire with various pool diameters from 0.2 m<sup>2</sup> to 1 m<sup>2</sup>.  
 194 Two liquid fuels commonly found in nuclear facilities are considered: Hydrogenated Tetra-  
 195 propylene (HTP) used for reprocessing processes and lubricating oil used for gas turbines.  
 196 Dodecane (has a similar chemical formulation to HTP), and heptane were also used for  
 197 comparison with other results in the literature [31].

198 Table 1. List of experiments and main results

Serie	Name	Pool area	Fuel type	Number of room	Number of Doorway	Number of vent	Fire room volume	Total Volume	Ventilation flow rate	Admission position	ACH	Extinction mode	Regime	$\dot{m}_f$	$\phi_o$	$\phi_m$	$t_{ext}$	$\dot{m}_f$
		(m <sup>2</sup> )		(#)	(#)	(#)	m <sup>3</sup>	m <sup>3</sup>	m <sup>3</sup> /h	(-)	(h <sup>-1</sup> )	(-)	(-)	(g/s)	(-)	(-)	(s)	(g/s)
SI	SI_D1	0.4	T	1	-	-	120	120	560	Top	4,67	O2	R2	13,2	1,10	1,67	3190	4,04
	SI_D2	0.4	T	1	-	-	120	120	1000	Top	8,33	F	R1	13,2	0,59	1,64	2580	6,02
	SI_D3	0.4	T	1	-	-	120	120	180	Top	1,50	O2	R3	13,2	2,84	1,67	360	12,25
	SI_D4	0.4	T	1	-	-	120	120	560	Top	4,67	O2	R2	13,2	1,03	1,65	2895	4,18
	SI_D5	0.2	T	1	-	-	120	120	560	Top	4,67	F	R1	5,3	0,43	0,75	2550	3,12
	SI_D5a	0.2	T	1	-	-	120	120	180	Top	1,50	O2	R2	5,3	1,15	0,82	1980	1,07
	SI_D6	0.4	T	1	-	-	120	120	560	Bot.	4,67	O2	R2	13,2	1,06	1,67	2500	6,40
SI_D6a	0.4	T	1	-	-	120	120	180	Bot.	1,50	O2	R3	13,2	6,80	1,65	560	8,18	
DOOR	DOOR1	0.4	T	2	1	-	120	240	50	Top	0,42	O2	R3	13,2	11,90	1,55	885	3,74
	DOOR2	0.4	T	2	1	-	120	240	180	Top	1,50	O2	R2	13,2	3,35	1,85	1410	4,83
	DOOR3	0.4	T	2	1	-	120	240	570	Top	4,75	F	R1	13,2	1,05	1,70	1910	7,88
	DOOR4	0.4	T	2	1	-	120	240	1000	Top	8,33	F	R1	13,2	0,61	1,57	1160	13,48
	DOOR5	1	T	2	1	-	120	240	570	Top	4,75	F	R1	40,8	3,26	1,66	1310	7,34
LK	LK_3	0.6	T	1	-	-	120	120	1850	Top	15,42	F	R1	21,9	0,59	1,84	1120	19,25
INT	INT_4	1	T	4	3	-	120	516	3100	-	25,83	F	R1	40,8	0,59	5,44	1610	30,09
VSP1	VSP_1A	0.3	H	1	-	-	120	120	2000	Top	16,67	F	R1	16,2	0,38	2,17	1555	13,08
VSP2	VSP_2	0.4	H	2	-	1	120	290	2320	Top	19,33	F	R1	23,7	0,46	2,88	1310	22,16
	VSP_3	0.4	H	2	-	1	120	290	960	Top	8,00	O2	R2	23,7	1,10	2,87	755	15,31
	VSP_4	0.4	H	2	-	1	120	290	960	Top	8,00	O2	R3	23,7	1,14	2,90	335	20,11
FES	FES_1	0.7	O	1	-	-	170	170	2550	Top	15,00	F	R1	16,3	0,29	1,86	2650	11,65
S3_3	S3_B0	0.56	D	3	1	-	120	360	1200	Top	10,00	F	R1	16,8	0,62	3,90	2650	14,05
	S3_C1	0.56	D	3	1	-	120	360	1200	Top	10,00	F	R1	16,8	0,65	3,89	3470	11,22
S3_4	S3_A1	0.4	O	4	1	1	120	530	10	-	0,08	F	R1	8,4	0,75	1,76	3620	5,33
	S3_A2	1	O	4	1	1	120	530	2400	Top	20,00	F	R1	24,5	0,49	8,85	6250	16,09

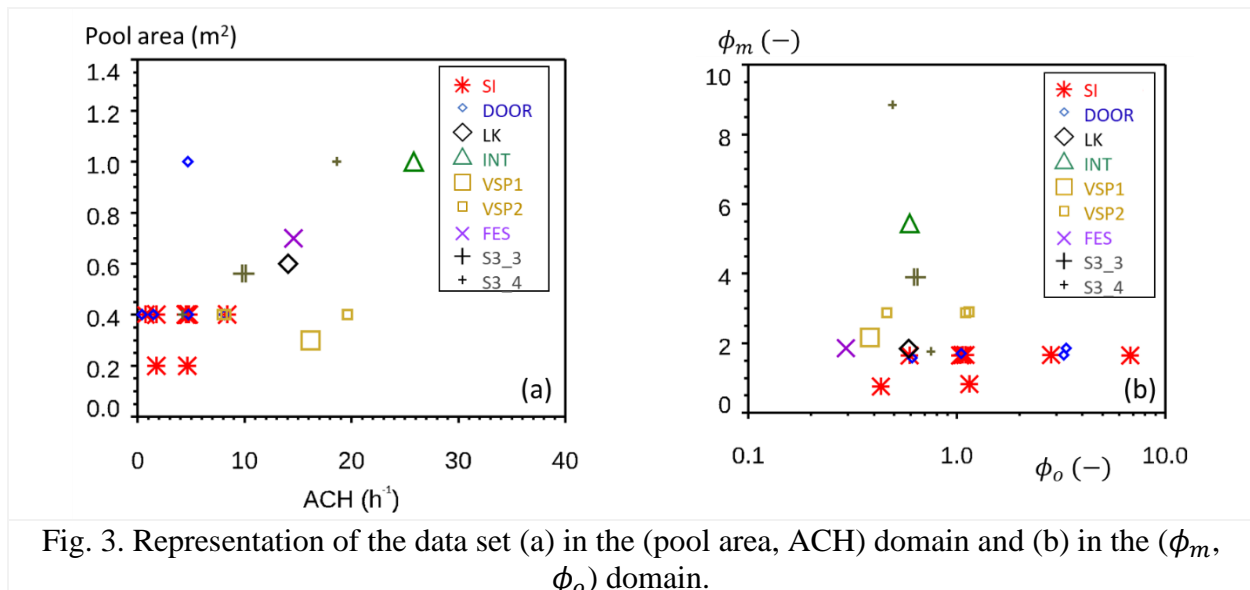
199 T=TPH ; H=Heptane - O=Lub.oil - D=Dodecane - O2= lack of oxygen - F=lack of fuel

200 The test parameters are given in Table 1. These are the pool size (from 0.2 m<sup>2</sup> to 1 m<sup>2</sup>), the fuel  
 201 type (HTP, heptane, dodecane and lubricant oil), the number of rooms, the size of the fire room,  
 202 the presence of openings in the fire room (doorway or vent), the ventilation flow rate or ACH  
 203 induced by the mechanical ventilation only and the position of the air intake (Bottom or Top).

204 One of the aims of this study is to show the influence of the ventilation on the MLR for a wide  
 205 variety of ventilation configurations that are representative of real-life situations.

206 All the tests were carried out in the same facility and the instrumentation used was identical. The  
 207 mass loss was measured by a SARTORIUS balance located under the pan. The measurement  
 208 range was 300 kg with an accuracy of 2 g. Ventilation flow rates were measured by ANNUBAR  
 209 type averaged Pitot probes inserted in the ventilation ducts and connected to pressure  
 210 transducers. The volume flow rate was obtained by considering the ANNUBAR probe  
 211 coefficient and the gas temperature. The uncertainty on the volume flow rate was assessed to  
 212 10%. Oxygen concentrations were measured by SERVOMEX XANTRA 4100 gas analysers  
 213 fitted with paramagnetic cells. These analysers were connected to a sampling case that takes gas  
 214 samples at three points in the fire compartment (at the top at 0.85 m from the ceiling, at the  
 215 bottom at 1 m from the ground and near the fire at the pan level on its side). The uncertainty on  
 216 oxygen concentration was assessed as less than 1%. The MLR is obtained as the time derivative  
 217 of the mass loss signal. The extinction time is determined visually and consolidated with the  
 218 mass loss measurement. The mode of extinction (through lack of oxygen or lack of fuel) is  
 219 determined based on the fuel mass. More detailed information for each campaign can be found in  
 220 the references dedicated to modelling (SI, [25]-[26], DOOR, [27], LK, [28], INT, [29], VSP1 and  
 221 VSP2, [20], FES, [30]).

222 All the tests are shown in the domain (pool area, ACH) illustrating the ranges considered for the  
 223 two parameters (Fig. 3-a). As suggested by the WSR model, the tests can be represented in the  
 224 ( $\phi_m, \phi_o$ ) domain (see Fig. 3-b). The  $\phi_m$  factor is greater than 0.7 which indicate that the mass of  
 225 fuel was large enough to investigate the effect of the ventilation and the ventilation factor  $\phi_o$  is  
 226 well-distributed over a wide range including well- and under-ventilated regimes.





## 227 3 Results

### 228 3.1 Behaviour in open atmosphere

229 Fuels were characterized in an open environment under a calorimetric hood in order to determine  
230 the evolution of MLR per unit of area ( $\dot{m}''$ ) in open environment with the pool diameter  $D$ . This  
231 quantity is needed to determine the MLR in an open environment  $\dot{m}_f^o = \pi D^2/4 \times \dot{m}''$  used in the  
232 evaluation of the ventilation factor  $\phi_o$  introduced in the section 2.1. The MLR per unit of area  
233 can be theoretically expressed with Babrauskas's relationship,  $\dot{m}''(D) = \dot{m}_{\infty}''(1 - \exp(-k\beta D))$   
234 where  $\dot{m}_{\infty}''$  and  $k\beta$  are the two parameters characterizing the constant MLR per unit area for large  
235 diameters and the propensity to produce soot. For the four fuels, experiments are carried out with  
236 several diameters to obtain the parameters  $\dot{m}_{\infty}''$  and  $k\beta$  from fitting. The results given in Fig. 4,  
237 agree with the theoretical prediction and the parameters agree with those found in the literature  
238 [32]. The variability of the results also observed in the literature [33] is due to the influence of  
239 initial and boundary conditions such as ambient temperature, initial fuel height or pan height.  
240 The results also show that heptane is, among the four, the fuel that leads to the highest MLR for  
241 a given diameter while HTP and Dodecane have similar results, and lubricant oil has the lowest  
242 MLR. Both HTP and Dodecane fuel give similar results. Lubricant oil is the fuel giving the  
243 lowest MLR.

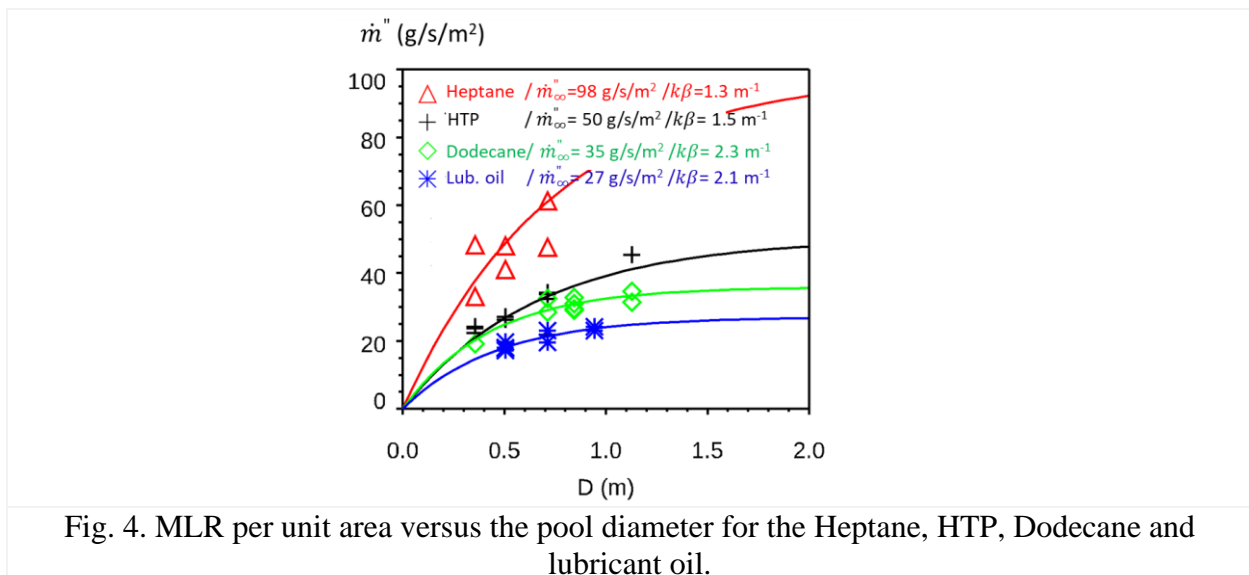


Fig. 4. MLR per unit area versus the pool diameter for the Heptane, HTP, Dodecane and lubricant oil.

### 244 3.2 Influence of environmental conditions

245 The wide variety of configurations studied during the PRISME projects highlights the influence  
246 of environmental conditions on the MLR. Three parameters have been studied: the ventilation  
247 rate, the presence of an opening (in this case a doorway) and the position of the inlet. The aim  
248 here is to study whether the influence of these parameters, highlighted on a reduced or  
249 intermediate scale, can be found on a large scale in real configurations. Firstly, configurations  
250 involving a single mechanically ventilated compartment (SI and VSP1 campaigns) are

251 considered. The major effect of the ventilation flow rate decrease is a reduction of the MLR in  
 252 comparison to the level in open atmosphere. As shown in Fig. 5-(a) and (b), after a transitory  
 253 phase during which a behaviour like that in open environment is observed, a stationary behaviour  
 254 is evidenced, for which the average MLR is lower than the one in open environment. Lower the  
 255 ventilation flow rate and lower the MLR. This result is reported whatever the pool area ( $0.2 \text{ m}^2$   
 256 or  $0.4 \text{ m}^2$  Fig. 5 (a) and (b)) or the nature of the fuel (HTP or Heptane Fig. 5 (c)). This result  
 257 agree with literature as for example the work of Peatross & al. [1]. One consequence is a longer  
 258 fire duration in comparison to that in open atmosphere if extinction occurs through lack of fuel.  
 259 In case of a low, and potentially limited ventilation rate, extinction occurs rapidly when the LOI  
 260 is reached, and the fire duration becomes very short ( $\text{ACH}=1.7 \text{ h}^{-1}$  in Fig. 5 (b) or  $\text{ACH}=7.8 \text{ h}^{-1}$   
 261 in Fig. 5 (c)). The test series with heptane also show oscillatory behaviour of the MLR that may  
 262 appear for low values of the ventilation rate (Fig. 5 (c)). The results obtained on a large scale also  
 263 confirm the observation made on a reduced scale [7], [16]. The oscillations appear for conditions  
 264 leading to oxygen concentrations close to the extinguishing conditions. Modulations of the MLR  
 265 are associated with those of the air intake into the compartment, induced by a coupling between  
 266 the fire heat release rate and the ventilation network. The effect of the ventilation flow rate is  
 267 also observed on more complex configurations with two rooms. The fire room is ventilated  
 268 mechanically but also naturally with the doorway. Similar results as those obtained with one  
 269 room are reported Fig. 5-(d)). The main difference is that a steady state is no longer achieved.  
 270 The MLR decreases progressively until extinction.

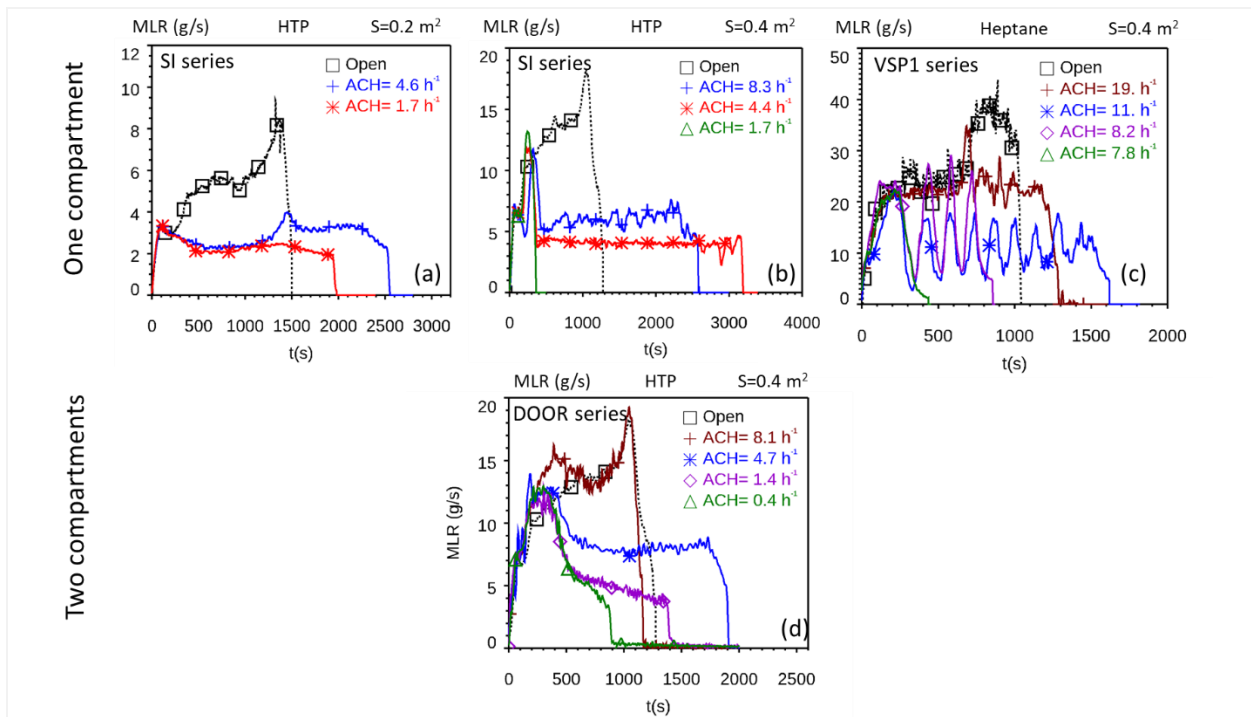


Fig. 5. Effect of the ventilation flow rate on the MLR time variation for two configurations: one compartment (first line) (a) with  $0.2 \text{ m}^2$  HTP pool fires (b) with  $0.4 \text{ m}^2$  HTP pool fires (c) with  $0.4 \text{ m}^2$  heptane pool fire; and two compartments (second line) (d) with  $0.4 \text{ m}^2$  HTP pool fires

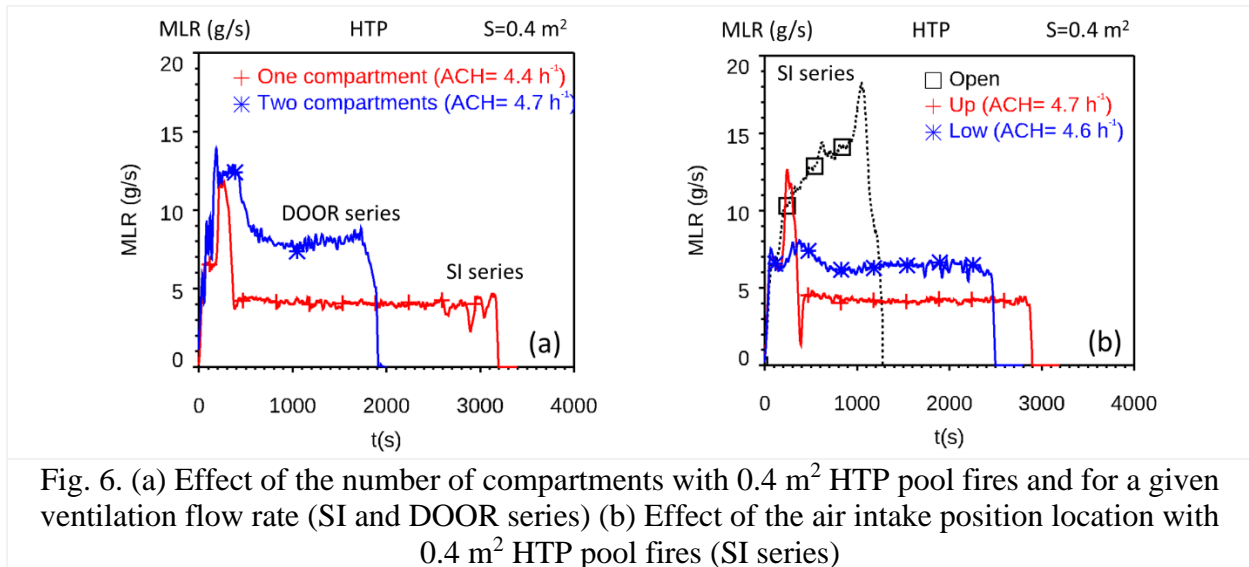


Fig. 6. (a) Effect of the number of compartments with  $0.4 \text{ m}^2$  HTP pool fires and for a given ventilation flow rate (SI and DOOR series) (b) Effect of the air intake position location with  $0.4 \text{ m}^2$  HTP pool fires (SI series)

271 It is important to note that different behaviours are observed for the same ventilation rate.  
 272 Indeed, the ventilation rate is not the only parameter influencing the classification of the tests  
 273 (and in the following section, the ventilation factor is introduced for this purpose), the nature of  
 274 the fuel (stoichiometric coefficient in particular), the type of ventilation (forced only or forced  
 275 with an open door) and the position of the air supply also have an influence. This is the reason  
 276 why different behaviours can be observed for the same ventilation flow rate value.

277 The effect of the presence of a doorway is isolated by comparing two similar tests (same fuel,  
 278 same mechanical ventilation rate and same fire compartment size) (Fig. 5-(e)). The results show  
 279 a greater MLR with a doorway compared to the same configuration without a doorway. The  
 280 doorway induced a significant incoming air flow which can be assessed with the relation  
 281  $0.5 \times A\sqrt{H}$  (where  $A$  and  $H$  are the section and the height of the opening). For standard  
 282 dimensions ( $H=2.1 \text{ m}$  and  $w=0.8 \text{ m}$ ), this air flow rate is in the range from 2,000 to 3,000  $\text{m}^3/\text{h}$   
 283 which corresponds to an ACH greater than  $15 \text{ h}^{-1}$  for a fire compartment of  $120 \text{ m}^3$ . Although  
 284 this result is expected, it is new and has received little attention in the literature.

285 The tests of these data-base were also able to highlight the influence of the position of the air  
 286 intake on the MLR. For a given configuration with only the air inlet as a variable parameter, the  
 287 MLR is higher for a low position, which is favourable for maintaining a high oxygen  
 288 concentration near the fire location (Fig. 5-(f)). The high position of the air intake is less efficient  
 289 for feeding the fire. These result agrees with a medium scale study that discussed this effect in a  
 290  $25 \text{ m}^3$  compartment [14]. The present tests confirm the significant effect of the position of the air  
 291 intake on the MLR. The tests at a large scale and for complex scenarios validate the results on  
 292 the influence of the fire scenario on the MLR, which to date have mainly been carried out on a  
 293 reduced or intermediate scale.

### 294 3.3 Combustion regimes and time to extinction

295 Based on the MLR temporal variation, three combustion regimes reported at small-scale in [10]  
296 are also considered here: regime 1 (R1), where the MLR experiences a stationary period with an  
297 amplitude lower than the level in open atmosphere but extinction occurs through lack of fuel,  
298 regime 2 (R2), where the MLR also shows a stationary period with an amplitude lower than the  
299 level in open atmosphere but extinction occurs through lack of oxygen (there is still fuel in the  
300 pan after extinction), and regime 3 (R3), where the MLR shows a transient period and extinction  
301 rapidly occurs through lack of oxygen (the limit oxygen index, LOI, is reached). For a given  
302 scenario, these three regimes are correlated to the value of the ventilation factor,  $\phi_o$  as predicted  
303 by the WSR model. Regimes R1, R2 and R3 are respectively observed successively when  $\phi_o$   
304 increases.

305 A second parameter of interest is the duration of the combustion phase. As observed for the  
306 MLR temporal variation, the vitiation of the surrounding environment can lead to different  
307 behaviours of the duration versus the ventilation flow rate; either an increase due to the decrease  
308 of the MLR or a decrease due to a rapid extinction through lack of oxygen. This behaviour, also  
309 highlighted with the WSR model, is analysed from these large scale data-base. For each test, the  
310 duration of the combustion phase, the mode of extinction (through lack of fuel, F or lack of  
311 oxygen O) as well as the combustion regime (R1, R2 and R3) are identified and the ventilation  
312 factor  $\phi_o$  and a dimensionless time  $t_{ext}^*$  determined (Table 1). As defined previously, the  
313 ventilation factor is computed from the MLR in open atmosphere and only from the mechanical  
314 ventilation flow rate in the fire compartment before ignition.

315 The dimensionless time versus the ventilation factor is presented in Fig. 7 for each scenario  
316 indicating also and the type of combustion regime (R1, R2 and R3). On each plot, the data and  
317 the WSR predictions are compared. For the three scenarios corresponding to series SI, DOOR  
318 and VSP2, enough tests have been performed to visualize the three regimes and to observe  
319 similar behaviour to that predicted theoretically. The increase of the dimensionless fire duration  
320 with the ventilation factor corresponds to regime 1. Regime 3 corresponds to the opposite  
321 behaviour for higher values of  $\phi_o$ . Regime R2 corresponds to the transitional regime between the  
322 two behaviours. A critical ventilation factor can be experimentally determined, respectively  
323 about 1.11, 3.43 and 1.11 for the series SI, DOOR and VSP2. A comparison with the WSR  
324 model is proposed, considering the experimental parameter  $\phi_m$  and adjusting realistic values for  
325  $M^e$  and  $Y^e$  to obtain the value of the critical ventilation factor that enables the model to reproduce  
326 the data as well as possible. The values of  $M^e$  and  $Y^e$  are summarized in Table 2. Results show  
327 very similar trends, highlighting the suitability of the WSR approach for reproducing the test  
328 results. It is worth noting that for the scenario including doorway (DOOR), the parameters ( $M^e$ ,  
329  $Y^e$ ) need to be modified to move the critical ventilation factor,  $\phi_o^c$ , toward a larger value (about  
330 3) and to fit the data. For the other configurations, for which only one regime R1 is evidenced,  
331 the critical ventilation is only assessed by fitting the WSR predictions.

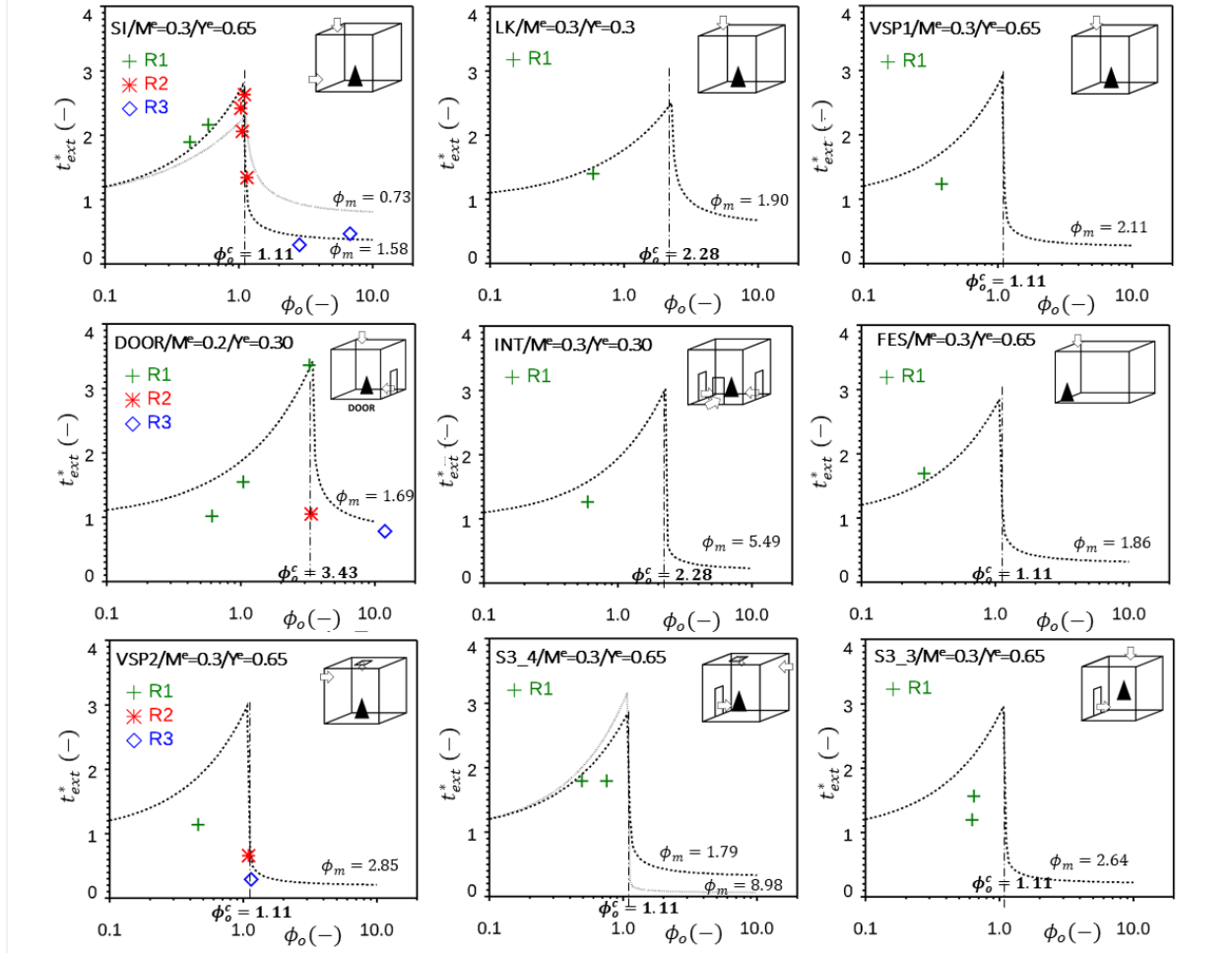


Fig. 7. Dimensionless time to extinction versus the ventilation factor for each configuration (first line) mechanical ventilation only (second and third lines) mechanical ventilation and natural ventilation with doorway and vent

332  
333

Table 2. Values of  $M^e$  and  $Y^e$  and the corresponding critical ventilation factor used for the prediction with the WSR model.

	SI	FES	LK	INT	VSP1	VSP2	FES	S3_3	S3_4	NYX
$M^e$	0.3	0.2	0.3	0.3	0.3	0.3	0.3	0.3	0.3	0.44
$Y^e$	0.65	0.3	0.3	0.3	0.65	0.65	0.65	0.65	0.65	0.76
$\phi_o^c$	1.11	3.43	2.28	2.28	1.11	1.11	1.11	1.11	1.11	0.51

334

335 Despite the optimisation of the critical ventilation factor, in some cases there are discrepancies  
 336 between the experimental points and the model. These discrepancies are attributed more to the  
 337 simplicity of the model than to experimental uncertainties. The experimental variables, in this  
 338 case the duration of the combustion phase and the initial fuel mass, have a fairly low uncertainty.

339 The fact that there are different  $\phi_o^c$  values between the configurations is explained by the  
 340 contribution of the openings (doorway or vent) to the global effect of the ventilation. The  
 341 presence of openings in addition to mechanical ventilation leads to a shift in the observed trend  
 342 towards higher values of the ventilation factor. The ventilation factor as it is defined in the WSR  
 343 model is a global parameter that does not include the specific nature of each configuration and in  
 344 particular the additional effects of openings to the oxygenation of the fire.

345 Nevertheless, a generic behaviour can be proposed by scaling the ventilation factor by its critical  
 346 value (Fig. 8). Despite the different configurations, the combustion regimes can be classified  
 347 according to the value of the ventilation factor. For values below the critical value, the duration  
 348 of the fire increases with the normalised ventilation factor due to the decrease in MLR; the  
 349 duration of the combustion phase can increase up to three times the duration in an open  
 350 environment (tests from all campaigns). For ventilation factor values higher than a critical value,  
 351 the duration of the fire is lower than in open environment because of anticipated extinction  
 352 through lack of oxygen (tests from SI and DOOR campaigns). Between these two regimes, there  
 353 is a transition stage, during which the duration can take very variable values for the same  
 354 ventilation factor corresponding to the critical value (tests from SI, DOOR and VSP2). A  
 355 comparison with tests carried out on a reduced scale single compartment without opening ([10])  
 356 shows very similar behaviour, illustrating the generic nature of this representation. For this test  
 357 series, the critical ventilation factor was 0.52 [10]. This evolution of the dimensionless time  
 358 versus the ventilation factor scaled by the critical ventilation factor is generic to fire scenarios of  
 359 different scales, various types of ventilation and various hydrocarbon fuels. It also allows  
 360 ranking of the three combustion regimes. The critical ventilation factor is therefore a good  
 361 indicator for characterising a fire scenario. The higher it is, the more the scenario favours  
 362 oxygenation of the fire.

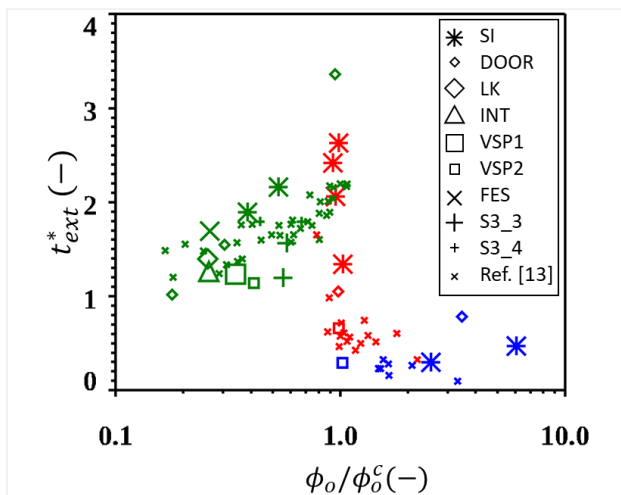


Fig. 8. Dimensionless time to extinction versus the ventilation factor scaled by its critical value (Regime R1 in green, regime R2 in red and regime R3 in blue)

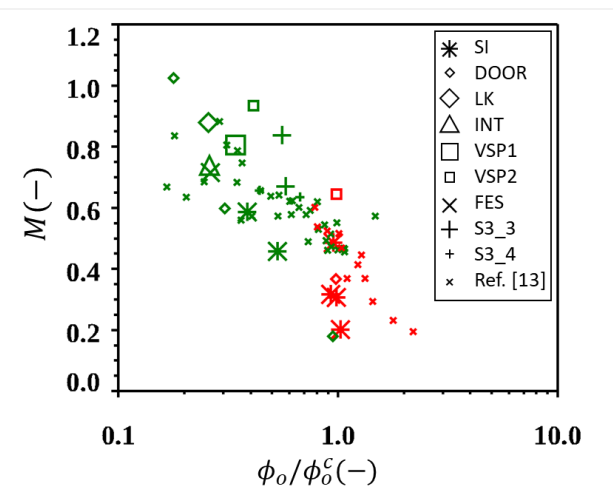


Fig. 9. Dimensionless MLR versus the ventilation factor scaled by its critical value (Regime R1 in green and regime R2 in red)

363 It is worth noting a non-negligible spread of the points around a common trend. This dispersion  
364 is explained by the fact that the ventilation factor is a global parameter, which does not allow the  
365 specific features of each scenario (shape of the enclosure, position of the air inlets, position of  
366 the fire location, etc.) to be considered. For the same ventilation factor and the same initial mass  
367 of fuel, the duration of the fire can be slightly different.

368 Theoretical analysis shows that the critical ventilation factor depends on the extinction  
369 conditions (minimum MLR at extinction and LOI). The prediction of these scenarios in regime  
370 R2 is most complex because it requires satisfactory modelling of the extinction conditions that  
371 may be different for each test. On the other hand, for scenarios with a small or very large  
372 ventilation factor, any inaccuracy in the extinction conditions will have no (regime R1) or little  
373 (regime R3) influence on the prediction.

### 374 **3.4 Burning rate in vitiated environment**

375 The WSR model also highlights that the decrease in MLR is correlated with the ventilation  
376 factor. This analysis is conducted on tests with a R1 or R2 combustion regime for which a  
377 stationary phase is identified. The results, presented in Fig. 9, show indeed a decrease in MLR as  
378 a function of ventilation factor. This result demonstrates the influence of the oxygen  
379 concentration on the MLR. As the ventilation factor increases and consequently the oxygen  
380 concentration decreases, the MLR decreases. This result is evidence that there is a need in the  
381 model of a relationship between the MLR and the oxygen concentration. A general trend is  
382 observed for all the large-scale tests as well as for the reduced-scale experiments, indicating the  
383 generic character of this result. Nevertheless, as with the study of the fire duration, dispersion of  
384 the experimental data is evidenced (Fig. 9). It is also explained by the global character of the  
385 ventilation factor but also by the uncertainty in the identification of the stationary phase for  
386 which the MLR is assessed.

387 One relationship of interest is that between the MLR and the characteristics of the surrounding  
388 environment. To identify this relation and to validate the relationship introduced in the WSR  
389 model with relation (3), these quantities measured during the tests are evaluated for a stationary  
390 phase and only for the tests on regime R1 or R2. The correlation between MLR and oxygen  
391 concentration is presented in Fig. 10. The results show a decrease in MLR with oxygen  
392 concentration, as expected. A comparison with the specific Peatross & Beyler law, relation (3)  
393 with  $M^e=0$  and  $Y^e=0.53$ , shows good agreement for some tests. For other tests, the experimental  
394 points are far from the theoretical prediction. This can be explained in two ways. The first  
395 concerns the experimental difficulty in obtaining a concentration representative of the average  
396 concentration of the flows used to oxidize the combustible. Defining the control volume over  
397 which the oxygen concentration should be assessed is difficult for some scenarios. In these cases,  
398 the global approach reaches its limits and a detailed CFD approach (with adapted combustion  
399 and pyrolysis models) seems to be necessary. The second point concerns the influence of  
400 induced flows as well as external heat fluxes, which will contribute to increasing the MLR  
401 despite low oxygen concentration. This is the case for the LK and INT tests where the fire  
402 compartment was highly thermally insulated, resulting in a high temperature overall. The VSP2  
403 and INT tests concern scenarios with the presence of openings, reinforcing the MLR. For these

404 tests, relationship (3) including only the effect of oxygen is incomplete. The influence of  
 405 additional effects such as heat flux and induced flows must be integrated.

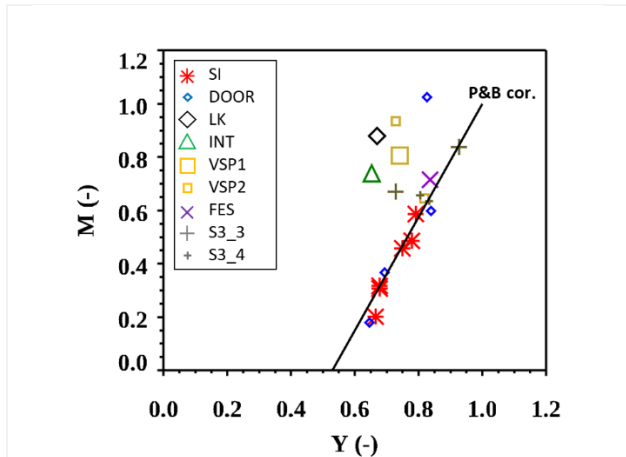


Fig. 10. Relationship between the dimensionless MLR and oxygen concentration near the fire location at steady state

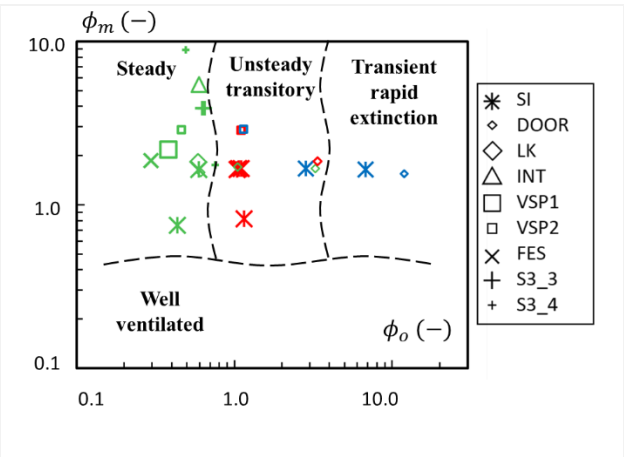


Fig. 11. Classification of fire scenario in a  $(\phi_o, \phi_m)$  map with the PRISME project tests as examples (Regime R1 in green, regime R2 in red and regime R3 in blue)

406 Nevertheless, the good agreement in average of the relation (3) correlation explains why this  
 407 relationship, widely used in simulation tools, may give satisfactory results for some scenarios.  
 408 However, the results also show that for scenarios close to the extinction conditions and in the  
 409 presence of additional effects to that of oxygen (external flow, temperature, flow), this relation  
 410 needs to be improved.

### 411 3.5 Classification of the fire scenario

412 By analysing the large-scale fire test data-base with the theoretical support of the WSR model, a  
 413 classification of the fire scenarios can be made based on two parameters, the ventilation factor  
 414  $\phi_o$  and the mass factor  $\phi_m$ . Depending on the values taken by these two parameters, the fire  
 415 scenarios can be sorted according to their behaviour (Fig. 11). For  $\phi_m$  values below a limit  
 416 estimated from the simulations to be about 0.6, the fire scenarios are not very sensitive to the  
 417 ventilation rate (and thus to the ventilation factor) due to a small amount of fuel in a large  
 418 volume; these scenarios can be similar to those in an open environment. For values of  $\phi_m$  greater  
 419 than the above-mentioned limit, the ventilation and in particular the ventilation flow rate  
 420 (expressed through  $\phi_o$ ) influences the fire scenario by reducing the burning rate compared to its  
 421 value in open atmosphere. For low values of  $\phi_o$ , the MLR is reduced by the vitiation of the  
 422 surrounding environment, the duration of the combustion phase is longer than in an open  
 423 environment and extinction occurs due to lack of fuel. The LOI limit is never reached. On the  
 424 other hand, for large values of  $\phi_o$ , the MLR is also reduced but extinction occurs quickly due to  
 425 lack of oxygen (the LOI is reached) and the duration of the combustion phase is shorter than that  
 426 obtained in open environment. Between these two regimes, an intermediate regime is observed in  
 427 which the MLR also decreases, and the oxygen concentration stabilises at values close to the



428 LOI. These regimes correspond to unstable situations during which oscillatory regimes can be  
429 observed. This mapping was obtained from both large- and small-scale tests and for a wide  
430 variety of vessel geometry configurations and four fuel types. It is important to mention that it is  
431 the area of unstable and transient behaviour that is the most difficult to predict and which  
432 requires greater attention in the future.

#### 433 **4 Conclusions**

434 This study presents an analysis of the effect of the environmental conditions on the MLR in case  
435 of mechanically ventilated compartments constituting complex and realistic fire scenarios with  
436 hybrid ventilation systems. The database used, produced during the PRISME projects, includes  
437 large-scale configurations involving several compartments with ventilation of the fire  
438 compartment combining mechanical ventilation and natural ventilation through openings  
439 (doorway or vent). The main objective was to analyse the behaviour of the MLR on these new  
440 data-base involving complex situations and to compare them with the results observed on  
441 reduced or intermediate scales and on simple ventilation configurations. The following  
442 conclusions were obtained.

443 A review of the WSR model highlighted the properties specific to fire scenarios in a  
444 mechanically ventilated compartment. The under-ventilated combustion regimes reported in  
445 mechanically ventilated enclosures can be classified using two parameters, the ventilation factor  
446  $\phi_o$ , and the mass factor  $\phi_m$ , both calculated from known variables. Depending on the value of  
447 these parameters, several combustion regimes are identified by comparing the MLR with that  
448 obtained in the open environment: either similar to the open environment, or weaker in the open  
449 environment with three particular situations: stationary, unstable or transient with rapid  
450 extinction. The WSR model also highlights the critical ventilation factor indicating the  
451 conditions under which ventilation regimes are obtained.

452 The well-stirred reactor model's interpretation, carried out to date on a reduced and intermediate  
453 scales (up to 38 m<sup>3</sup> compartment) or for simplified configurations, is also valid and robust for the  
454 PRISME projects data-base comprising complex configurations representative of real fire event  
455 (120 m<sup>3</sup> compartment with hybrid ventilation systems).

456 The different combustion regimes observed on a reduced scale are also found in complex  
457 scenarios. The duration of the combustion phase and the mass loss rate are strongly correlated  
458 with the ventilation factor normalised by its critical value. This generalisation to both small- and  
459 large-scale tests and to both simple and complex scenarios confirms the robustness of the  
460 interpretation.

461 The analysis of the law relating the MLR to environmental conditions is also found for the  
462 database studied. This result confirms the robustness of this law and thus explains why the  
463 simulation attempts for the PRISME project tests have generally given satisfactory results.  
464 However, the analysis also confirms that for certain configurations, this law needs to be  
465 improved, to take into account situations where the influence of external flows and temperature  
466 are non-negligible compared with the effect of oxygen. The analysis also shows that knowledge

467 of the conditions of extinction and its introduction into the models need to be improved in  
468 order to deal with regimes at the extinction limit.

469

## 470 **Acknowledgements**

471 The authors are grateful for the support of the members participating in the OECD/NEA  
472 PRISME, PRISME2 and PRISME3 projects.

## 473 **References**

- 474 [1] M. J. Peatross and G. L. Beyler, "Ventilation effects on compartment fire  
475 characterization," in *Fire Safety Science, Proceeding of the Fifth International*  
476 *Symposium*, 1997, pp. 403–414.
- 477 [2] S. Suard, P. Zavaleta, and H. Prétrel, "Overview of the OECD PRISME 3 Project," in *in*  
478 *Roewekamp, M. and Berg, H.P. (Eds) : Proceeding of SMiRT 25, 16th International*  
479 *Seminar on Fire Safety in Nuclear Power Plants and Installations, Kolen, Germany,*  
480 *December, 2019.*
- 481 [3] S. Suard, P. Van Hees, M. Roewekamp, S. Tsuchino, and R. Gonzalez, "Fire development  
482 in multi-compartment facilities: PRISME 2 project," *Fire Mater.*, vol. 43, no. 5, pp. 433–  
483 435, 2019, doi: 10.1002/fam.2754.
- 484 [4] L. Audouin, L. Rigollet, H. Prétrel, W. Le Saux, and M. Röwekamp, "OECD PRISME  
485 project : Fires in confined and ventilated nuclear-type multi-compartments - Overview and  
486 main experimental results," *Fire Saf. J.*, vol. 62, pp. 80–101, 2013, doi:  
487 10.1016/j.firesaf.2013.07.008.
- 488 [5] O. Sugawa, K. Kawagoe, Y. Oka, and I. Ogahara, "Burning Behavior in a Poorly-  
489 Ventilated Compartment Fire -Ghosting Fire-," *Fire Sci. Technol.*, vol. 9, no. 2, pp. 2\_5-  
490 2\_14, 1989, doi: 10.3210/fst.9.2\_5.
- 491 [6] Q. He, C. Li, S. Lu, C. Wang, and J. Zhang, "Pool Fires in a Corner Ceiling Vented Cabin:  
492 Ghosting Flame and Corresponding Fire Parameters," *Fire Technol.*, vol. 51, no. 3, pp.  
493 537–552, 2015, doi: 10.1007/s10694-015-0467-0.
- 494 [7] Y. Utiskul, J. G. Quintiere, A. S. Rangwala, B. A. Ringwelski, K. Wakatsuki, and T.  
495 Naruse, "Compartment fire phenomena under limited ventilation," *Fire Saf. J.*, vol. 40, no.  
496 4, pp. 367–390, 2005, doi: 10.1016/j.firesaf.2005.02.002.
- 497 [8] H. Prétrel, S. Suard, and L. Audouin, "Experimental and numerical study of low  
498 frequency oscillatory behaviour of a large-scale hydrocarbon pool fire in a mechanically  
499 ventilated compartment," *Fire Saf. J.*, vol. 83, pp. 38–53, 2016, doi:

- 500 10.1016/j.firesaf.2016.04.001.
- 501 [9] A. Nasr, S. Suard, H. El-Rabii, J. P. Garo, L. Gay, and L. Rigollet, “Heat feedback to the  
502 fuel surface of a pool fire in an enclosure,” *Fire Saf. J.*, vol. 60, pp. 56–63, 2013, doi:  
503 10.1016/j.firesaf.2012.12.005.
- 504 [10] H. Prétrel, N. Charaoui, B. Lafdal, and S. Suard, “Effect of environmental conditions on  
505 fire combustion regimes in mechanically-ventilated compartments,” *Fire Saf. J.*, vol. 127,  
506 no. June 2021, 2022, doi: 10.1016/j.firesaf.2021.103493.
- 507 [11] A. S. X. Loo, A. Coppalle, J. Yon, and P. Aîné, “Time-dependent smoke yield and mass  
508 loss of pool fires in a reduced-scale mechanically ventilated compartment,” *Fire Saf. J.*,  
509 vol. 81, pp. 32–43, 2016, doi: 10.1016/j.firesaf.2016.01.006.
- 510 [12] A. Nasr, S. Suard, H. El-Rabii, L. Gay, and J. P. Garo, “Fuel mass-loss rate determination  
511 in a confined and mechanically ventilated compartment fire using a global approach,”  
512 *Combust. Sci. Technol.*, vol. 183, no. 12, pp. 1342–1359, 2011, doi:  
513 10.1080/00102202.2011.596174.
- 514 [13] L. Acherar, H. Y. Wang, J. P. Garo, and B. Coudour, “Impact of air intake position on fire  
515 dynamics in mechanically ventilated compartment,” *Fire Saf. J.*, vol. 118, no. February, p.  
516 103210, 2020, doi: 10.1016/j.firesaf.2020.103210.
- 517 [14] S. Lu, R. Chen, B. Zhang, X. Wang, and C. Li, “Effects of Air Inlet Configuration on  
518 Forced-Ventilation Enclosure Fires on a Naval Ship,” *Fire Technol.*, vol. 52, pp. 547–562,  
519 2016, doi: 10.1007/s10694-015-0473-2.
- 520 [15] Y. Utiskul and J. G. Quintiere, “Generalizations on compartment fires from smallscale  
521 experiments for low ventilation conditions,” *Fire Saf. Sci.*, pp. 1229–1240, 2005, doi:  
522 10.3801/IAFSS.FSS.8-1229.
- 523 [16] M. Mense, Y. Pizzo, H. Prétrel, C. Lallemand, and B. Porterie, “Experimental and  
524 numerical study on low-frequency oscillating behaviour of liquid pool fires in a small-  
525 scale mechanically-ventilated compartment,” *Fire Saf. J.*, 2019, doi:  
526 10.1016/j.firesaf.2019.102824.
- 527 [17] D. Alibert, M. Coutin, M. Mense, Y. Pizzo, and B. Porterie, “Effect of oxygen  
528 concentration on the combustion of horizontally-oriented slabs of PMMA,” *Fire Saf. J.*,  
529 vol. 91, no. March, pp. 182–190, 2017, doi: 10.1016/j.firesaf.2017.03.051.
- 530 [18] H. Prétrel, B. Lafdal, and S. Suard, “Multi-scale analysis of the under-ventilated  
531 combustion regime for the case of a fire event in a confined and mechanically ventilated  
532 compartment,” *Fire Saf. J.*, 2020, doi: <https://doi.org/10.1016/j.firesaf.2020.103069>.
- 533 [19] W. Le Saux, H. Prétrel, C. Lucchesi, and P. Guillou, “Experimental study of the fire mass

- 534 loss rate in confined and mechanically ventilated multi-room scenarios,” in *Fire Safety*  
535 *Science*, 2008, pp. 943–954, doi: 10.3801/IAFSS.FSS.9-943.
- 536 [20] H. Prétrel and S. Vaux, “Experimental and numerical analysis of fire scenarios involving  
537 two mechanically ventilated compartments connected together with a horizontal vent,”  
538 *Fire Mater.*, vol. 43, no. 5, pp. 514–529, 2019, doi: 10.1002/fam.2695.
- 539 [21] S. Suard *et al.*, “Analytical Approach for Predicting Effects of Vitiated Air on the Mass  
540 Loss Rate of Large Pool Fire in Confined Compartment,” in *International Symposium of*  
541 *Fire Safety Science*, 2011, doi: DOI: 10.3801/IAFSS.FSS.10-1513.
- 542 [22] J. G. Quintiere, *Fundamentals of Fire Phenomena*. 2006.
- 543 [23] S. Melis and L. Audouin, “Effects of vitiation on the heat release rate in mechanically-  
544 ventilated compartment fires,” *Fire Saf. Sci.*, pp. 931–942, 2008, doi:  
545 10.3801/IAFSS.FSS.9-931.
- 546 [24] A. Snegirev, “Perfectly stirred reactor model to evaluate extinction of diffusion flame,”  
547 *Combust. Flame*, vol. 162, no. 10, pp. 3622–3631, 2015, doi:  
548 10.1016/j.combustflame.2015.06.019.
- 549 [25] H. Prétrel, P. Querre, and M. Forestier, “Experimental study of burning rate behaviour in  
550 confined and ventilated fire compartments,” in *Fire Safety Science*, 2005.
- 551 [26] J. F. Perez Segovia, T. Beji, and B. Merci, *CFD Simulations of Pool Fires in a Confined*  
552 *and Ventilated Enclosure Using the Peatross–Beyler Correlation to Calculate the Mass*  
553 *Loss Rate*, vol. 53, no. 4. Springer US, 2017.
- 554 [27] J. Wahlqvist and P. Van Hees, “Validation of FDS for large-scale well-confined  
555 mechanically ventilated fire scenarios with emphasis on predicting ventilation system  
556 behavior,” *Fire Saf. J.*, 2013, doi: 10.1016/j.firesaf.2013.07.007.
- 557 [28] S. Vaux and H. Prétrel, “Relative effects of inertia and buoyancy on smoke propagation in  
558 confined and forced ventilated enclosure fire scenarios,” *Fire Saf. J.*, vol. 62, pp. 206–220,  
559 2013, doi: 10.1016/j.firesaf.2013.01.013.
- 560 [29] D. Le, J. Labahn, T. Beji, C. B. Devaud, E. J. Weckman, and A. Bounagui, “Assessment  
561 of the capabilities of FireFOAM to model large-scale fires in a well-confined and  
562 mechanically ventilated multi-compartment structure,” *J. Fire Sci.*, vol. 36, no. 1, pp. 3–  
563 29, 2018, doi: 10.1177/0734904117733427.
- 564 [30] S. Vaux, H. Prétrel, and L. Audouin, “Experimental and numerical study of water spray  
565 system for a fire event in a confined and mechanically ventilated compartment,” *Fire*  
566 *Mater.*, vol. 43, no. 5, 2019, doi: 10.1002/fam.2719.

567 [31] J. Lassus, L. Courty, J. P. Garo, E. Studer, P. Jourda, and P. Aine, “Ventilation effects in  
568 confined and mechanically ventilated fires,” *Int. J. Therm. Sci.*, vol. 75, pp. 87–94, 2014,  
569 doi: 10.1016/j.ijthermalsci.2013.07.015.

570 [32] B. Merci and T. Beji, *Fluid Mechanics Aspects of Fire and Smoke Dynamics in*  
571 *Enclosures*. 2022.

572 [33] V. Babrauskas and S. J. Grayson, *Heat release in fires*. Interscience communications,  
573 1990.

574

575

576 **Figure captions**

577 Fig. 1. Examples of simulation with the WSR model (where  $Me=0.44$  and  $Ye=0.76$ ) (top) time  
578 variation of O2 concentration with  $\phi_m=0.2$ , (left) and with  $\phi_m=0.6$  (right)- (Bottom)  $t_{ext}^*$   
579 versus the ventilation factor  $\phi_o$  for three values of  $\phi_m$  (right), Iso-contours of  $t_{ext}^*$  in the  
580  $(\phi_m, \phi_o)$  domain.

581 Fig. 2. Illustration of the configurations considered in the PRISME projects (arrows indicate the  
582 air flows).

583 Fig. 3. Representation of the data set in the  $(\phi_m, \phi_o)$  domain.

584 Fig. 4. MLR per unit area versus the pool diameter for the Heptane, HTP, Dodecane and  
585 lubricant oil.

586 Fig. 5. Effect of the ventilation flow rate on the MLR time variation for various configurations  
587 (a) effect of the ACH with 0.2 m2 with HTP (b) effect of the ACH with 0.4 m2 with HTP (c)  
588 effect of the ACH with 0.4 m2 with heptane (d) effect of the ACH with 0.4 m2 with two  
589 compartment configuration - DOOR series, (e) effect of the opening SI and DOOR series (f)  
590 effect of the air intake position SI series.

591 Fig. 6. Dimensionless time to extinction versus the ventilation factor for each configuration (first  
592 line) mechanical ventilation only (second and third lines) mechanical ventilation and natural  
593 ventilation with doorway and vent

594 Fig. 7. Dimensionless time to extinction versus the ventilation factor scaled by its critical value  
595 (Regime R1 in green, regime R2 in red and regime R3 in blue)

596 Fig. 8. Dimensionless MLR versus the ventilation factor scaled by its critical value (Regime R1  
597 in green and regime R2 in red)

598 Fig. 9. Relationship between the dimensionless MLR and oxygen concentration near the fire  
599 location at steady state

600 Fig. 10. Classification of fire scenario in a  $(\phi_o, \phi_m)$  map with the PRISME project tests as  
601 examples